Growth Rate Biometric Quantification by X-ray Microtomography on Larger Benthic Foraminifera: Three-dimensional Measurements Push Nummulitids into the Fourth Dimension

ANTONINO BRIGUGLIO[1], BRIAN METSCHER[2] & JOHANN HOHENEGGER[3]

[1] Department of Palaeontology, University of Vienna, Geozentrum, Althanstrasse 14,
1090 Vienna, Austria (E-mail: antonino.briguglio@univie.ac.at)
[2] Department of Theoretical Biology, University of Vienna, Althanstrasse 14, 1090 Wien, Austria
[3] Department of Palaeontology, University of Vienna, Geozentrum, Althanstrasse 14, 1090 Vienna, Austria

Abstract: This work demonstrates the potential of three-dimensional biometric quantification using microtomography on larger benthic foraminifera. We compare traditional linear and area measures used for calculating three-dimensional characters with actual 3D measurements made from volume images obtained using X-ray microtomography (microCT).

Two specimens of recent larger benthic foraminifera, i.e., *Palaeonummulites venosus* and *Operculina ammonoides*, were imaged with a high-resolution microCT scanner. This method enables three-dimensional imaging and calculation of measurements like 3D distances, surfaces and volumes.

The quantitative high-resolution images enabled the extraction of the lumina from the proloculus to the last complete scanned chamber and of the canal system spreading into marginal chord and septa. External surfaces and volumes were calculated on the extracted parts. These measurements allowed the calculation of porosity and micro-porosity to obtain the test density, which is the basis for many inferences about foraminifera, e.g., reconstructions of transport and deposition. Volume and surface measurements of the proloculus allow the calculation of sphericity deviation, which is useful for determining evolutionary trends in species based on individuals resulting from asexual reproduction (A forms).

The three-dimensional data presented here show the actual growth of the foraminiferal cell and the development of the test. Measurements made on an equatorial section cannot be considered representative of a three-dimensional test, unless a correspondence between 2D data with 3D data shows significant correlation. Chamber height, septal distance, spiral growth and chamber area were measured on the equatorial section and correlated with the volume measurements from 3D images to determine the predictive value of the 1D and 2D measures for estimating the 3D morphological parameters.

In particular, we show that the equatorial section area of chambers correlates significantly with the chamber volume and can be used to differentiate between nummulitid genera according to their different growth patterns.

Key Words: larger benthic foraminifera, biometry, density, X-ray microtomography, volume calculation, phylogeny

İri Bentik Foraminiferlerde Gelişimin X-ray Mikrotomografisi ile Biyometrik olarak Tanımlanması: Nummulitidlerde Üç-boyutlu Çalışmalar Dördüncü Boyutu Zorlamakta

Özet: Bu çalışma, mikrotomoğrafi kullanarak iri bentik foraminiferlerin üç-boyutlu biyometrik tanımlanmasındaki potansiyeli irdelemekte olup, üç-boyutlu karakterlerin hesaplamasında kullanılan geleneksel doğrusal ve alan ölçümleri, X-ray mikrotomoğrafisinden (microCT) elde edilen üç boyutlu (3D) ölçümler ile karşılaştırılmıştır. Bu amaçla, güncel iki bentik foraminifer, *Palaeonummulites venosus* ve *Operculina ammonoides* yüksek çözünürlü microCT ile taranmış ve görüntüleri elde edilmiştir. Uygulanan yöntem üç boyutlu görüntülemeyi ve uzaklık, yüzey ve hacim gibi parametrelerin hesaplanmasına olanak vermektedir.

Yüksek çözünürlü sayısal görüntüler ilk loca'dan (prolokülüs) taranmış son locaya kadar tüm loca alanlarını ve kenarda olan (marjinal) kord ve septa'ya kadar uzanan kanal sistemlerini tanımlar ve dış alanlar ve hacimlerin hesaplanmasına olanak verir. Bu ölçümler, foraminifer kavkısının taşınması ve depolanması gibi konularda belirleyici etken olan kavkı yoğunluğu ve mikro gözeneklilik gibi parametrelerin hesaplamasında önemlidir. Prolokülüs'ün hacim ve yüzey ölçümleri türlerde megalosferik (A-formlar) formların evrimsel değişimi hakkında fikir veren küresellikten sapmanın hesaplanmasına olanak vermektedir. Üç boyutlu veriler foraminifer hücresinin büyümesi ve kavkı gelişimini

ortaya koymakta olup, ekvatoryal kesitlerde yapılan ölçümler 2D ve 3D verileri arasında belirgin bir korelasyon gözlenmediği sürece üç boyutlu kavkı için temsili değildir. Bunun için ekvatoryal kesitlerde loca yüksekliği, septalar arası uzaklık, spiral büyüme ve loca alanı gibi parametreler ölçülmüş ve sonuçlar 3D ile elde edilen hacim ölçüleri ile deneştirilmiştir.

Elde edilen veriler ekvatoryal kesitdeki alan ölçümlerinin loca hacmi ile korelasyon gösterdiğini ve bu kapsamda farklı gelişim modelleri sunan nummulitid cinslerinin ayırtlanabileceğine işaret etmektedir.

Anahtar Sözcükler: iri bentik foraminifer, biyometri, yoğunluk, X-ray mikrotomoğrafisi, hacim hesabı, filojeni

Introduction

Many earth science studies, especially in palaeontology, require examination or measurement of the internal features of specimens or rocks in three dimensions, tasks to which X-ray microtomography (microCT) is very well suited (Carlson *et al.* 2003). A variety of different X-ray CT instruments and techniques are now available: they can scan objects of a size range from less than one millimetre, to many decimetres and they can scan at different resolutions: from less than one micron ('nanoCT') to one or a few microns (microCT), and up to the submillimetre-millimetre range (CT). The best-known advantage of X-ray CT is its ability to reconstruct quickly and non-destructively the interior of opaque solid objects in three dimensions when the density contrast is high enough to let the X-ray differentiate the internal features (Neues & Epple 2008; Metscher 2009). For many fossils, X-ray CT may be the only practical means of gaining information on internal materials and geometries or other features hidden from external view (e.g., Speijer *et al.* 2008). The digital and quantitative nature of a CT dataset facilitates computer visualization, animation, allowing the user to interact with the data and to better understand the features and interrelationships among elements of the dataset. Finally, these digital data provide unrivalled means for archiving and exchanging information, always at high resolution with intrinsic spatial calibration.

Because 3D visualization techniques are computationally intensive, they have historically been restricted to professional workstations, preventing widespread use. However, recent advances in processing power and 3D graphics cards, along with inexpensive computer memory and hard drives, make 3D visualization of reasonably sized data sets feasible and affordable even for laboratories that face budget constraints. Although one can still usefully spend a huge amount of money on a dedicated imaging workstation, a standard modern desktop computer can now be adequate for most imaging tasks encountered in routine microscopy, and the many open source software packages available reduce the cost of the whole research effort.

With larger foraminifera, their highly complex shells are used as the basis of their systematics down to the sub-species level. According to Hottinger (2009), quantitative morphological characters that change with time in one direction define the interpretation of phylogenetic trends in some groups of larger foraminifera. Such morphological characters are normally studied on oriented thin sections. The availability of a high-resolution three-dimensional virtual model of specimens offers a key to evaluating such morphological characters within the complexity of form and shape. While the equatorial section allows the study of character changes during growth in two spatial dimensions, this is impossible for characters represented in the third dimension, such as chamber thickness etc. Here, the axial section shows only an incidental growth state and changes of these characteristics cannot be measured for each growth step. Thus, the task of a three-dimensional quantitative analysis on larger foraminifera is to test the significance of one- and two-dimensional data (such as the area) in comparison with 3D measurements (such as the chamber volumes). Because of the importance of all these morphological parameters for the microevolution, phylogenetic trends, palaeoecology and palaeoclimatology of larger benthic foraminifera, the study of their complex internal structure using microCT is even more essential. Speijer *et al.* (2008) have already discussed the potentiality of the high-resolution microCT, but calculating volume and equivalent radius only.

Our aim is to make another step forward to show the potential of the data obtained from 3D analysis:

quantification of volumes, surfaces, distances, angles and nearly any metrical feature of interest. Those data are still rare in many published papers describing microCT.

We have compared the data obtained by the X-ray computed tomography with classic biometry in nummulitids, which has a long history partially based on many parameters and some contradictions. As suggested by Schaub (1981) and widely used in many papers, the main morphological parameters used to describe megalospheric specimens of larger benthic foraminifera are the major and minor diameter, the morphology and number of septa per whorls and the diameter of the proloculus. Other parameters (in particular the radii of the whorls) do not seem useful in order to understand the growth process (Pecheux 1995). Other authors (e.g., Roveda 1970) used to determine nummulitids lineage relying mainly on the external test shape, diameter, thickness, and ornamentation. Further studies (e.g., Reiss & Hottinger 1984; Hallock & Glenn 1986; Racey 1992; Pecheux 1995) agreed that these features are largely influenced by environmental parameters, such as depth, substrate, light intensity, etc; hence they are important to obtain information about the palaeoecology and palaeogeography of larger foraminifera. According to Hottinger (2009), the only feature that may be quantified by simple linear measurement is the diameter of the megalospheric proloculus if it is a walled sphere; but among the possible species-diagnostic characters, all require the observation of the equatorial section.

Measuring and quantifying the foraminiferal cell growth rate with a three-dimensional analysis is the first step into the fourth dimension.

Material and Methods

Two A-form specimens with excellent test preservation were investigated. The *Operculina ammonoides* (Gronovius 1781) specimen originates from muddy substrate in 18 m depth of the lagoon west of Motobu Town, Motobu Peninsula, Okinawa, Japan (Hohenegger *et al.* 1999). The specimen of *Palaeonummulites venosus* (Fichtel & Moll 1798) originates from 50 m depth in front of a patch reef along the investigated depth transect A between

Seoko Jima and Minna Jima, Okinawa, Japan (Hohenegger *et al.* 1999), where the sea floor consists of medium-grained sand.

Three-dimensional analyses of more specimens or entire populations will provide much more information on volume variability and chamber morphologies, but today these procedures are too much time consuming.

Procedure

The X-ray microtomography system used in this work is model MicroXCT from Xradia Inc., Concord, CA (www.xradia.com) in the Theoretical Biology Department at the University of Vienna, Austria. This scanner uses a Hamamatsu L9421-02 tungsten X-ray source with an anode voltage between 20 and 90 kV, power between 4 and 8 W, and a spot size of 5 to 8 μm. The scanner configuration allows fields of view from 5 mm down to less than 500 μm. The X-ray projection image is formed on a scintillator crystal, made in-house by Xradia. The optical emissions of the scintillator is then imaged by a Nikon microscope objective lens onto a 1k × 1k CCD camera (Pixis, Princeton Instruments) cooled to −55° C to reduce dark noise. The optical imaging of the scintillator allows a final magnification independent of the geometric magnification of the X-ray projection imaging, and a final image resolution that is not limited by the X-ray source spot size. Several different optical objective lenses allow selection of the final magnification, while adjustments to the source-sample and sample-detector distances can be made to change the geometric magnification of the sample image on the scintillator. Projection images are collected automatically over 180° of rotation and horizontal slices through the sample are reconstructed automatically by the supplied Xradia software. Reconstruction parameters can be adjusted and the reconstruction repeated if necessary. The scanning system integrated control computer carries out these operations and is also used for viewing the reconstructed volumes and exporting image stacks in standard formats (e.g., TIFF).

The foraminifera samples were scanned in small cylindrical plastic containers (a polypropylene pipette tip or a Lego® round brick 1×1). Most

plastics are relatively transparent to X-rays and so are suitable for scanning mineralised specimens. Imaging parameters for the scans reported here are summarized in Table 1.

The computer used for manipulating the image stacks was equipped with an Intel®Core (TM)2 Quad CPU Q9400 at 2.66 GHz, 8 GB of RAM with a Microsoft Windows XP Professional x64 system provided by the Department of Palaeontology in the University of Vienna, Austria.

In this work ImageJ (http://rsbweb.nih.gov/ij) was used, which is perhaps the most popular open-source imaging software in neuroscience, for measurements of 2D images and basic visualization of 3D dataset through plugins including Volume Viewer (http://rsb.info.nih.gov/ij/plugins/volume-viewer.html) and VolumeJ (http://webscreen.ophth.uiowa.edu/bij/vr.htm). Image Surfer (another free program; http://cismm.cs.unc.edu/) was used for volume rendering, quantifications, slicing at arbitrary orientation, measurements in 2D and 3D and taking snapshots suitable for publication. Many other 3D visualization software packages could be used for these purposes: some are commercial and quite expensive for an academic department, such as Amira (www.amiravis.com) or Analyze (www.analyzedirect.com), but others are open source and they all support conventional stereoscopic 3D display technologies.

After reading the reconstructed image stack into the measuring software and after calibrating it with the correct voxel size (three-dimensional pixel size), we could extract with the lasso tool in ImageJ every single chamber using some manual modification. In fact, because the chambers are interconnected in several locations, each chamber was artificially closed at the beginning of every connection by a boundaries editing operation. If the goal of the operation is to calculate the volume of every lumen, this solution does not cause inaccuracy of data because foramina or stolons are not part of the chamber volume itself. On the contrary, if the goal is to calculate the exact porosity, calculation of the whole canal system (septal and marginal), the stolons and the chambers connections is mandatory.

Because the foraminifera scanned are Recent, their preservation is excellent and the microCT images were able to clearly demonstrate the density contrast between the hollow chambers and the calcitic test itself. Such preservation allowed seeing the whole canal system in the marginal chord and inside every septum; stolons are also visible. With the possibility of measuring volumes of such empty space within every septum and within the marginal chord, it was also possible to calculate the real density of the specimens. Taking into account that the voxel size is about 4 μm, this can also be considered as the highest inaccuracy value in linear measurements. For areas or volumes calculated from linear measurements, the uncertainty range is propagated to the second and to the third powers.

As well as volumes, many other values were calculated to permit comparison of our new data with those existing in the literature. These are areas of lumina (A), chamber length (or septal distance, l), chamber height (h) and spiral distance. All these parameters were taken on the virtual equatorial section (Figure 1). The thin section was obtained by using the slice extractor tool in Image Surfer, which allowed us to cut the specimens in every possible way; a tool like this is extremely helpful in the case of specimens that are not perfectly straight and have a curved periphery where a 'mechanical thin section'

Table 1. Technical settings of the X-ray microtomography system used during the specimen scanning.

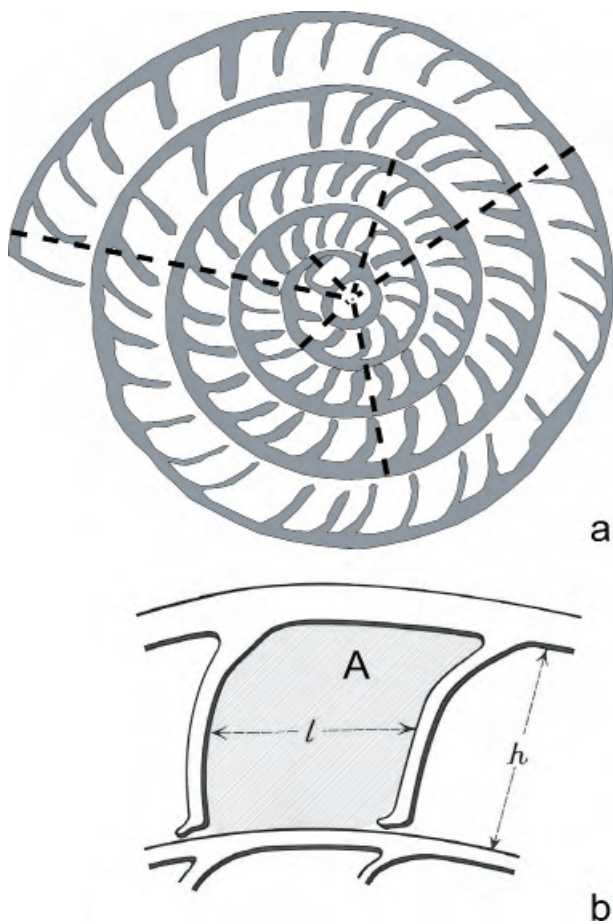|	*Palaenummulites Venosus*	*Operculina ammonoides*
Camera binning	2 X 2	2 X 2
Camera temperature	−55°C	−55°C
Image size	510 X 512	504 X 512
Clean file size	66.3 Mb	43.3 Mb
Anode voltage kV$_P$	80	77
μA	46	45
Source to RA distance	40.0 mm	40.0 mm
Detector to RA distance	22.0 mm	15.0 mm
Voxel	4.258 mA	4.645 mA
Optical magnification	4.2x	4.2x
Slides	268	174

Figure 1. **(a)** Sketch of the equatorial section of a nummulitid: the dotted lines show how the spiral distance was measured (modified from Briguglio & Hohenegger 2009); **(b)** detail of the equatorial section, with explanation how to measure the chamber height h, septal distance l and chamber area A (modified after Blondeau 1972).

is not reliable. To be rigorous in comparing the volumetric data with linear measurements or area calculations, the latter were upgraded to the third power in order to become comparable with volumes. Only in the comparison between volume and spiral form, were the volume data downgraded to one dimension.

Results

Each lumen was manually extracted from the proloculus to the last completely scanned chamber, so that volume and surface could be calculated for every chamber. The extracted chambers of *O.*

ammonoides and *P. venosus* are shown in Figure 2, and the measurements used in this work are reported in Table 2. A two-dimensional visualization of the three-dimensional dataset is not easy; for simplification, the extracted chamber lumina are illustrated whorl-by-whorl in equatorial and axial view and always at the same magnification. The last row in Figure 2 shows all the extracted chambers within the test.

The canal system was isolated both along the marginal chord and within the septa; the volume of this hollow space was calculated and added to the volumes of lumina to get an exact value of the total empty space inside the test.

Subtracting porosity (chamber lumina) and micro-porosity (canal system, stolons and foramina) from the total test volume, we get the volume of the test wall. This value allows the calculation of density, which is very important for calculating different transport effects. In *O. ammonoides* the 47 chambers' lumina represent 38% of the total volume. A total of 4.5% of the test wall is empty because of the canal system (marginal chord), which increases up to 9.6% when the septa are included. This porosity reduces the test wall volume to 53% of the total volume and may reduce density from 1.69 g/mm^3 down to 1.46 g/mm^3 including micro-porosity of the pores.

For *P. venosus*, the volume of all chambers represents 28% of the entire test (i.e. the marginal chord and septa are relatively thicker than in *O. ammonoides*) and the total porosity is 10% (against 15% in *O. ammonoides*); such values let test density reduce from 1.95 g/mm^3 to 1.75 g/mm^3.

The progression of lumina with test growth displays the ontogeny of the cell body. Such information may be used to detect or expect the reproduction stage in foraminifera (Hemleben *et al.* 1989). The embryonic apparatus was also extracted and separately compared (see Figure 3b). In the megalospheric generation of larger benthic foraminifera, the proloculus size and its connection with the deuteroconch is one of the main parameters for reconstructing phylogenetic trends (Less & Kovacs 1996; Papazzoni 1998).

The relation between growth rates of *P. venosus* and *O. ammonoides* is shown in Figure 3. The volumes of chamber lumina are presented both as an overview (Figure 3a) and whorl-by-whorl to study growth rate in detail (Figure 3c–f). Of
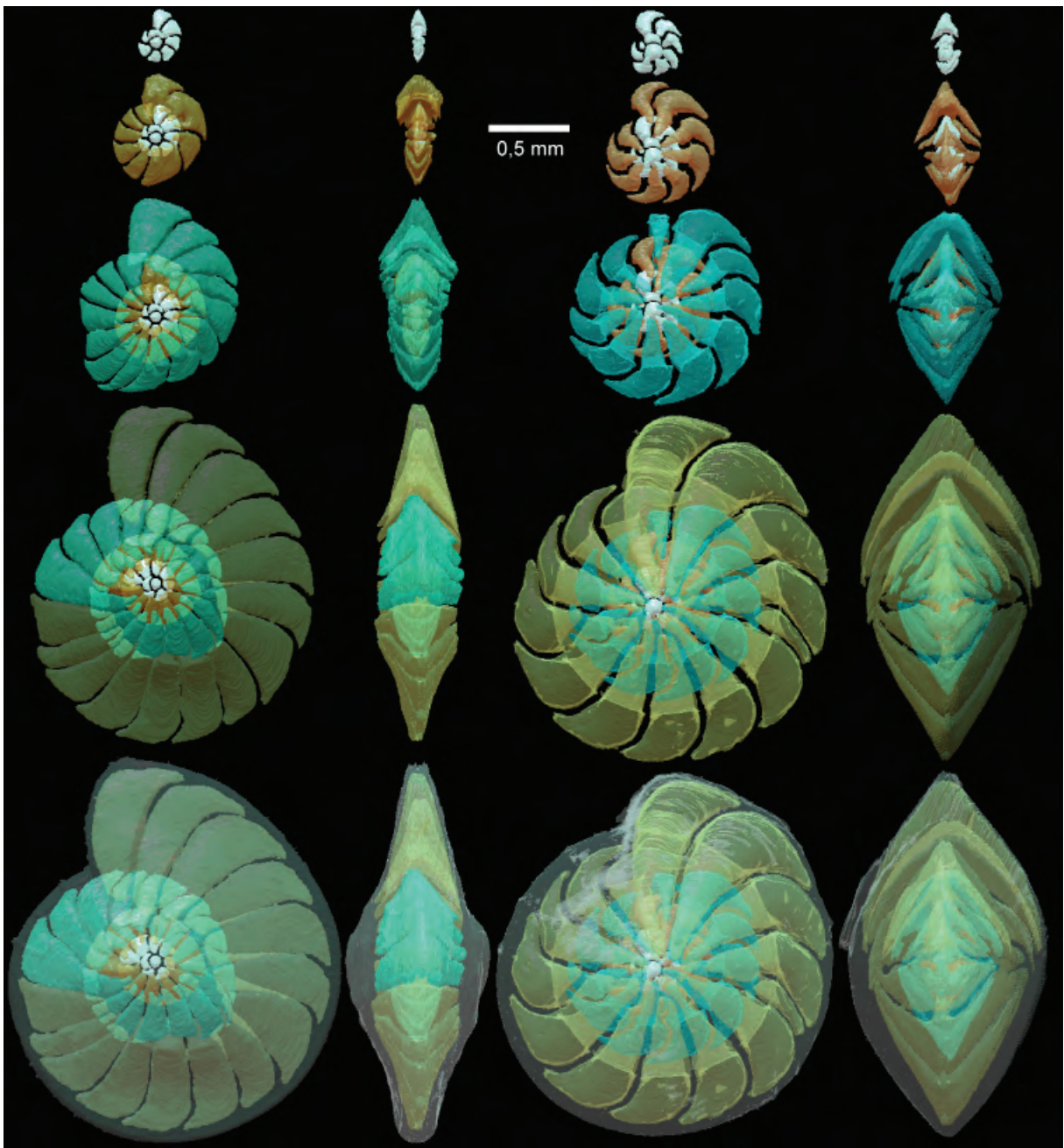
Figure 2. Three-dimensional representation of the chamber lumina, whorl after whorl, in equatorial and axial section of *O. ammonoides* (left side) and *P. venosus* (right side). The last row shows the lumina within the complete test.

course, the representation of the first whorl does not include proloculus and deuteroloculus, but starts actually from the consecutive chamber, then the first chamber after the embryonic apparatus. All values can be represented by an exponential function. In the first whorls, the exponential rate is high, but in the very last whorl, especially in the last four chambers showing reduced increase, the adult stage seems to be reached and reproduction might be possible; the algebraic function switches from an exponential to a logistic one, very commonly indicating the adult stage in foraminifera.

Table 2. Data obtained by measurements of the chamber lumen.

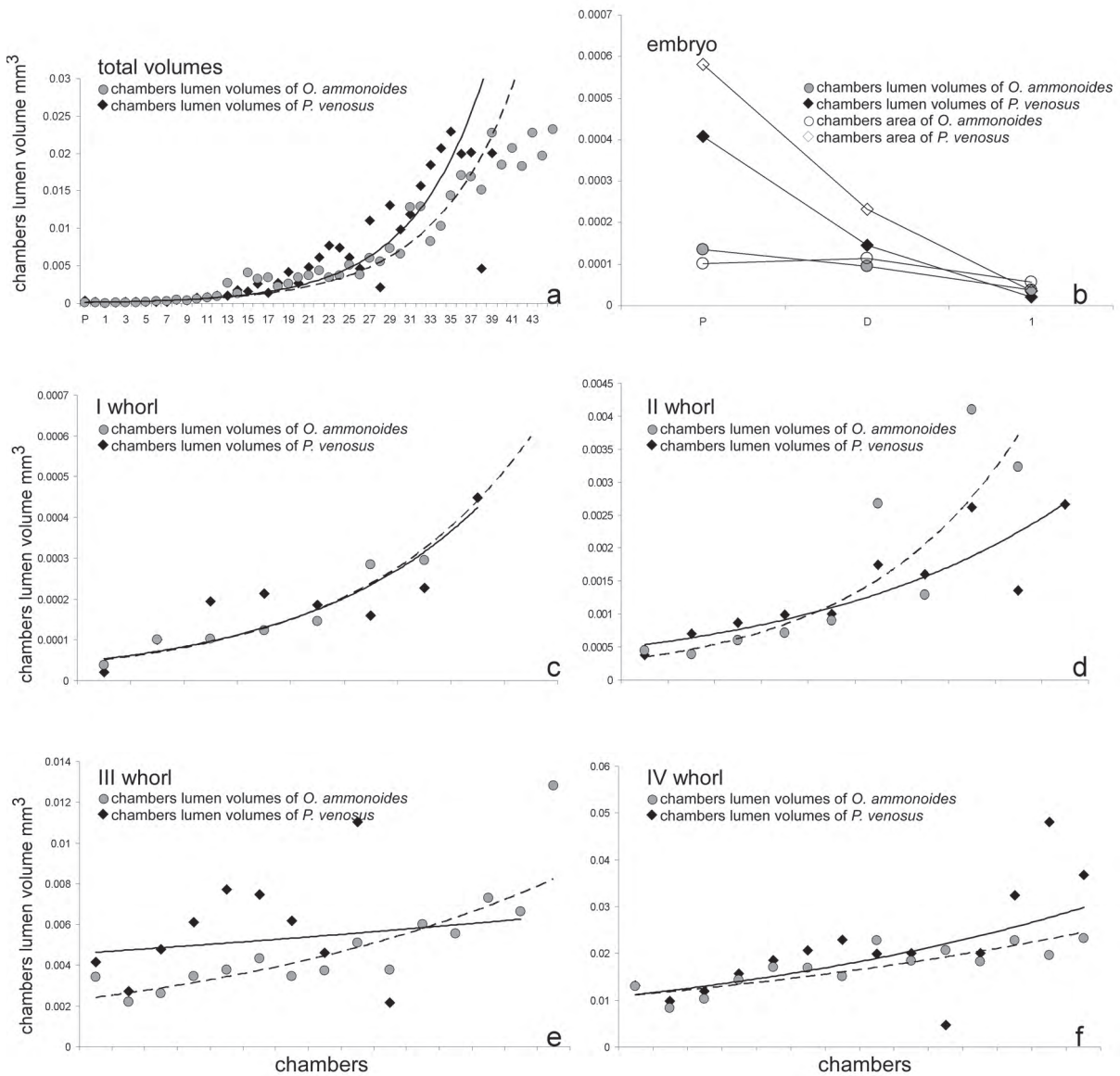| chamber	Volume cubic mm P. venosus	Volume cubic mm O. ammonoides	Chamber surface square mm P. venosus	Chamber surface square mm O. ammonoides	Chamber area square mm P. venosus	Chamber area square mm O. ammonoides	Septal distance mm P. venosus	Septal distance mm O. ammonoides	Chamber height mm P. venosus	Chamber height mm O. ammonoides	Spiral distance mm P. venosus	Spiral distance mm O. ammonoides
P	0.000409	0.000136	0.029563	0.014184	0.006961	0.00217521	0.089	0.066	0.048	0.037	0.123	0.107723
1	0.000146	0.000096	0.017026	0.01319	0.003774	0.002340357	0.03	0.032	0.034	0.045	0.113	0.11609
2	0.000021	0.000038	0.004301	0.006844	0.001106	0.001477222	0.055	0.055	0.059	0.054	0.158	0.12551
3	0.0001	0.0001	0.014205	0.013438	0.003065	0.003299745	0.061	0.058	0.064	0.064	0.155	0.1297
4	0.000195	0.000102	0.023554	0.012914	0.003763	0.0034328	0.074	0.057	0.057	0.064	0.152	0.151634
5	0.000214	0.000124	0.024848	0.015209	0.003592	0.00357764	0.068	0.061	0.058	0.08	0.172	0.1694
6	0.000186	0.000146	0.024609	0.016646	0.004721	0.00380635	0.082	0.075	0.057	0.073	0.161	0.209515
7	0.00016	0.000284	0.023671	0.027499	0.004095	0.005229585	0.08	0.078	0.059	0.075	0.231	0.23314
8	0.000228	0.000295	0.030986	0.026844	0.004491	0.006119652	0.086	0.08	0.091	0.089	0.259	0.259
9	0.000448	0.000448	0.045938	0.035602	0.009507	0.00653568	0.086	0.064	0.066	0.102	0.272	0.266126
10	0.000384	0.000391	0.04413	0.034273	0.005196	0.00562887	0.103	0.081	0.093	0.109	0.29	0.2769
11	0.000705	0.000603	0.063374	0.047506	0.008954	0.006442	0.102	0.08	0.085	0.101	0.294	0.294195
12	0.000864	0.000712	0.076743	0.056689	0.007474	0.11274	0.101	0.081	0.107	0.123	0.3	0.31219
13	0.000986	0.000904	0.085652	0.062558	0.012232	0.010381	0.106	0.216	0.087	0.137	0.324	0.292014
14	0.000998	0.002675	0.083245	0.147301	0.010268	0.020123	0.142	0.157	0.102	0.107	0.362	0.289526
15	0.001744	0.001287	0.12085	0.084985	0.013121	0.014995	0.12	0.252	0.119	0.102	0.392	0.351859
16	0.001607	0.004099	0.123931	0.211189	0.012741	0.02869	0.169	0.156	0.13	0.108	0.412	0.415904
17	0.002616	0.003229	0.166694	0.16008	0.024948	0.019628	0.1	0.135	0.129	0.152	0.446	0.469867
18	0.001356	0.003414	0.10707	0.159639	0.017167	0.02002	0.143	0.092	0.142	0.154	0.496	0.510169
19	0.002662	0.0022	0.176236	0.119462	0.02694	0.01485	0.184	0.092	0.131	0.146	0.536	0.516349
20	0.004154	0.002611	0.234941	0.130729	0.024765	0.1915	0.149	0.104	0.145	0.135	0.537	0.45108
21	0.00272	0.003441	0.172897	0.1601	0.021891	0.0214	0.186	0.124	0.148	0.127	0.526	0.484451
22	0.0048	0.00376	0.296796	0.184062	0.031753	0.01578	0.201	0.121	0.177	0.204	0.531	0.574595
23	0.006095	0.004325	0.303458	0.207899	0.046577	0.02359	0.211	0.095	0.233	0.196	0.557	0.532311
24	0.007714	0.003448	0.35213	0.188593	0.052798	0.013975	0.227	0.157	0.195	0.144	0.638	0.474102
25	0.007471	0.003744	0.360852	0.218934	0.054198	0.0216	0.185	0.199	0.199	0.127	0.676	0.4582
26	0.00617	0.005087	0.307388	0.298329	0.035753	0.02175	0.161	0.133	0.178	0.127	0.686	0.4607
27	0.004618	0.003762	0.243966	0.204892	0.031476	0.016355	0.256	0.171	0.16	0.126	0.688	0.533993
28	0.011035	0.005991	0.481937	0.269852	0.051074	0.023644	0.079	0.113	0.056	0.159	0.504	0.556742
29	0.002178	0.005554	0.190077	0.282918	0.005032	0.018869	0.192	0.137	0.182	0.18	0.709	0.592623
30	0.013112	0.007306	0.591864	0.31969	0.047517	0.030308	0.198	0.126	0.171	0.23	0.761	0.62813
31	0.009868	0.006636	0.445598	0.291719	0.045313	0.035919	0.3	0.195	0.156	0.265	0.772	0.718246
32	0.01192	0.012814	0.531496	0.440857	0.048023	0.06282	0.315	0.206	0.198	0.28	0.81	0.78219
33	0.015667	0.012897	0.536248	0.411679	0.055171	0.062528	0.3	0.129	0.229	0.298	0.817	0.824735
34	0.0185	0.008269	0.723119	0.329046	0.063209	0.036789	0.284	0.193	0.294	0.326	0.823	0.9004
35	0.020688	0.010323	0.701908	0.391059	0.068671	0.061133	0.284	0.194	0.307	0.391	0.831	0.950315
36	0.022984	0.014377	0.757051	0.460644	0.071143	0.089025	0.297	0.184	0.292	0.475	0.869	1.002945
37	0.01995	0.017044	0.713578	0.523607	0.068165	0.100209	0.308	0.182	0.305	0.46	0.941	1.030484
38	0.02012	0.0169	0.734502	0.516959	0.080886	0.09345	0.075	0.173	0.24	0.399	0.951	1.013711
39	0.00461	0.015125	0.29962	0.472946	0.017296	0.072675	0.251	0.22	0.214	0.408	0.968	0.982405
40	0.020016	0.022718	0.735222	0.635489	0.067414	0.11559	0.293	0.178	0.238	0.471	0.984	0.966269
41	0.032389	0.018461	1.049385	0.588321	0.09317	0.092785	0.37	0.211	0.312	0.487	1.002	0.912848
42	0.048042	0.020728	1.287386	0.618464	0.118972	0.119296	0.335	0.207	0.262	0.448	0.972	1.002482
43	0.03685	0.018313	1.318982	0.55896	0.084064	0.091201		0.285		0.45		0.983716
44		0.022767		0.702759		0.120728		0.208		0.482		1.044728
45		0.019664		0.591652		0.1096488		0.199		0.494		1.06
46		0.02325		0.623384		0.124131						

Figure 3. (a) Correspondence between chamber lumen volumes of *P. venosus* and *O. Ammonoides*: the functions are calculated as exponential; **(b)** correspondence between chamber lumen volumes and areas of the first three chambers (P, D, 1) of the two specimens; **(c–f)** chamber lumen volumes correspondence, whorl after whorl, of the two specimens. Continuous lines are exponential functions for the *P. venosus* set of data; dashed lines are exponential functions for the *O. ammonoides* set of data. All areas were recalculated as the cubic power to make them comparable with volume.

Therefore, chamber volume trends appear to be comparable with other nummulitids, i.e., tending to have an inflection point at the adult stage. In Figure 3b, proloculus (P), deuteroloculus (D) and first chamber (1) volumes are plotted and compared with their areas, measured on the equatorial section of the 3D image. Because of the identical slopes, the study of the embryonic stages in equatorial sections might be representative for the three-dimensional embryo.

Area calculation and its comparison with volumes also gives interesting results. As shown in Figure 4, the growth trend of the area is very similar to the volume growth rate in both investigated specimens.
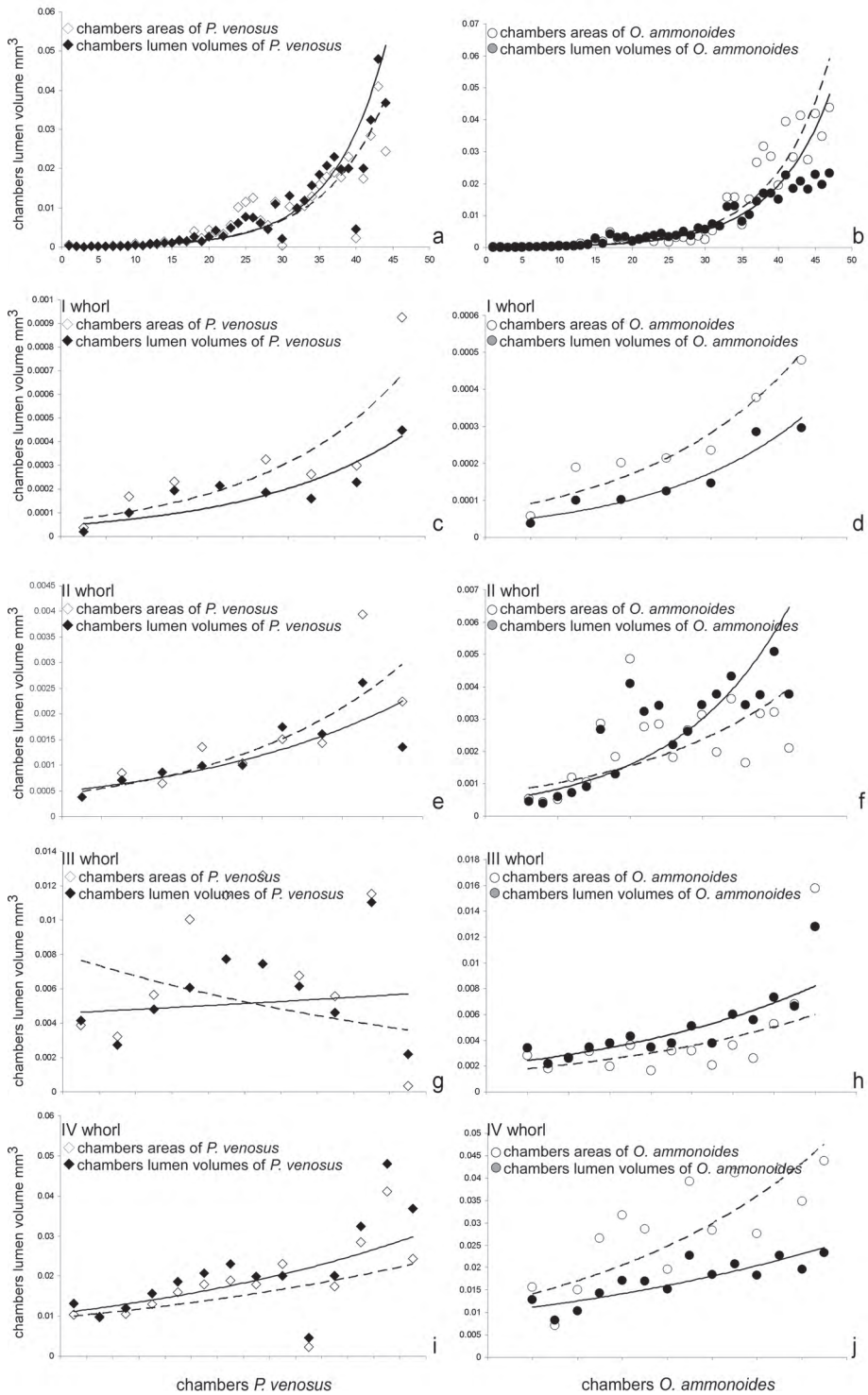
Figure 4. **(a)** correspondence between chamber lumen volumes of *P. venosus* and its areas; **(b)** correspondence between chamber lumen volumes of *O. ammonoides* and its areas; **(c, e, g, i)** correspondence between chamber lumen volumes and areas, whorl after whorl, of *P. venosus*; **(d, f, h, j)** correspondence between chamber lumen volumes and areas, whorl after whorl, of *O. ammonoides*. Continuous lines are exponential functions for the *P. venosus* set of data; dashed lines are exponential functions for the *O. ammonoides* set of data. All areas were recalculated as the cubic power to make them comparable with volume.

Because of different chamber morphologies between the two specimens, the areas in *O. ammonoides* are more similar to their volumes. Because the alar prolongations of *O. ammonoides* are shorter than in *P. venosus*, area calculation by equatorial section is more representative in operculinids (sensu Hottinger 1997) than in taxa, where alar prolongations can reach the umbilical boss. In the last whorl of *O. ammonoides* the calculation of the volume based on the area

$$v_i = \left(\sqrt{a_i} \right)^3$$

tends to overestimate the real volume because of the elevated chamber heights (see Figure 4 j).

In thin sections, we might have the impression that operculinids should possess higher growth rates than nummulitids, but the data obtained here seem to show a different trend: the growth rate measured by volumes does not have the same behaviour as chamber height (Figures 5 & 6). As discussed later, the chamber height, which grows faster in operculinids than in other nummulitids, produces such effects in thin section.

Comparing the growth of chamber length and height (Figures 5 & 6) with volumes, differences in chamber morphology becomes distinct. An estimate of the main ontogenetic trend is given for the first two whorls. In the last whorls, the chamber length is not significant for *P. venosus* and is underestimated (bigger whorl after whorl, Figure 5f, h, j) for *O. ammonoides*. The growth rate in chamber height (Figure 6) is consistent with the volume growth in *P. venosus*, but definitely overestimated in *O. ammonoides* (Figure 6j).

The relation between spiral and volume growth rates is shown in Figure 7. The data were recalculated to be comparable, i.e., volume data were transformed to linear data by cubic root to compare this trend with spiral growth, and these functions were calculated as linear and forced to intersect the origin (Figure 7a, b). This comparison gave us information about growth related to biological need (volume for protoplasm growth) compared to chamber geometry. In both *P. venosus* and *O. ammonoides* the spiral has a higher growth rate than the linearized volume. The different chamber morphology of the two specimens affects the spiral growth, which is in fact very similar,

whorl-by-whorl, in both taxa. No inflection points were observed in spiral growth, as expected close to the proposed reproduction status in volume growth.

The deviation from sphericity is illustrated in Figure 8. The correspondence between volume surface ratio and linear volume is reported for both specimens (see Figure 8a), but nothing seem to differentiate the two linear growths. Using the calculation proposed by Wadell (1932) with the following equation was more successful:

$$\psi = \frac{\pi^{\frac{1}{3}} (6V)^{\frac{2}{3}}}{S}$$

where *V* and *S* are the chamber volume and the chamber surface respectively. Using this formula, the range limits are given by 0 (e.g., surface without volume) and 1 (e.g., perfect sphere).

In both specimens the proloculi have a value slightly exceeding 0.9 and can be considered as spheres, but after the first two whorls showing a decrease, sphericity seems to reach stable values close to 0.5 for *P. venosus* and 0.6 for *O. ammonoides*.

Because of the good correspondence between volume and area, regressions were calculated for *P. venosus* and *O. ammonoides* to see the power of statistical correlations. As shown in Figure 9 the best fit for *O. ammonoides* is represented by a linear regression (forced through the origin), but this is not the best solution for *P. venosus* in which the best fit is represented by a power regression with an exponent > 1.

Discussion

The calculation from 3D images of chamber volumes and shapes and their changes during ontogeny gives a huge amount of information quite impossible to obtain by the traditional two-dimensional methodology of oriented thin section. The volume measure gives no information about shell geometry but indicates the influence of temporal changes during foraminiferal growth.

Mathematically, the construction of a chamber possessing a specific volume has an infinite number of solutions; but the evolved morphogenetic solutions
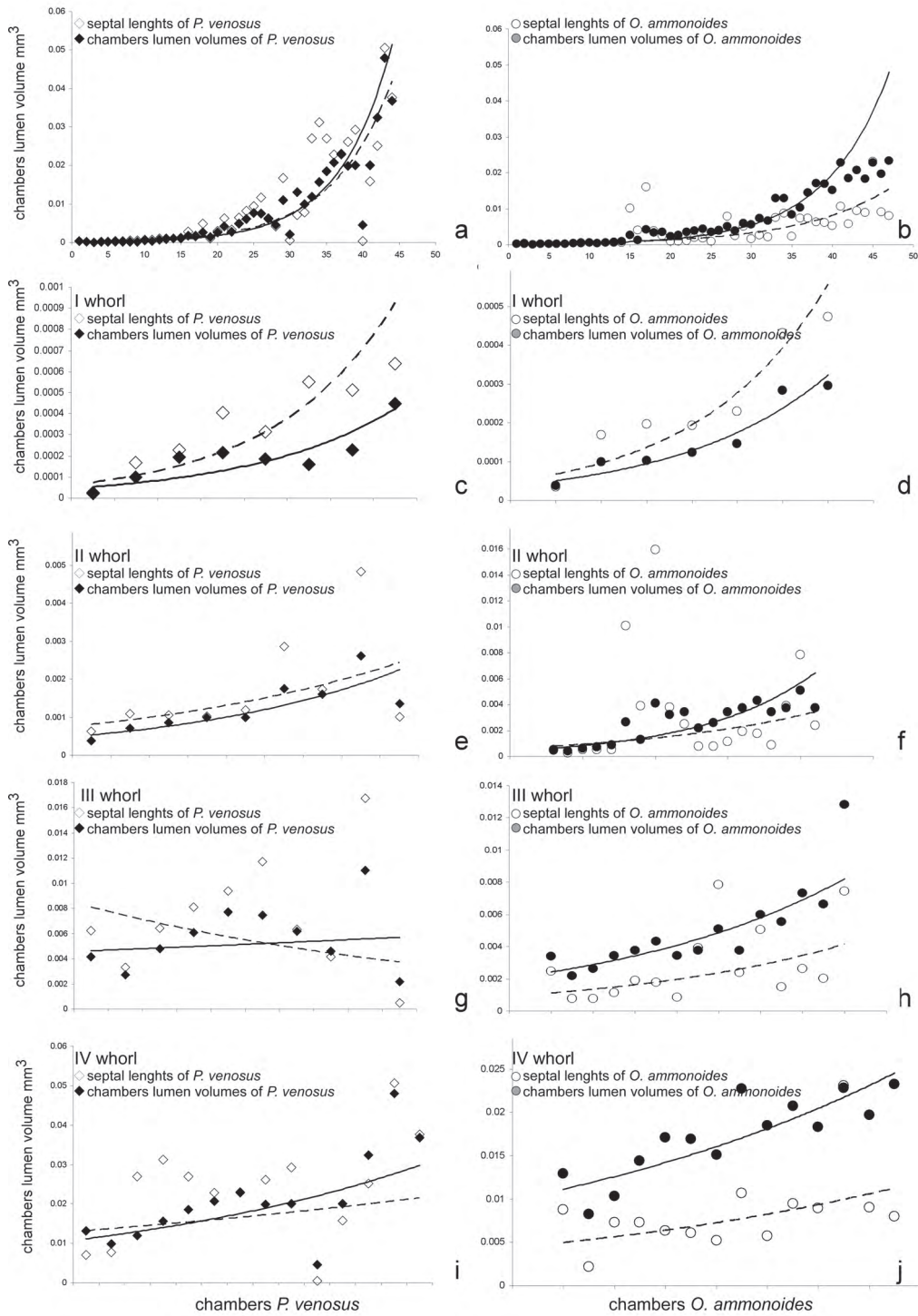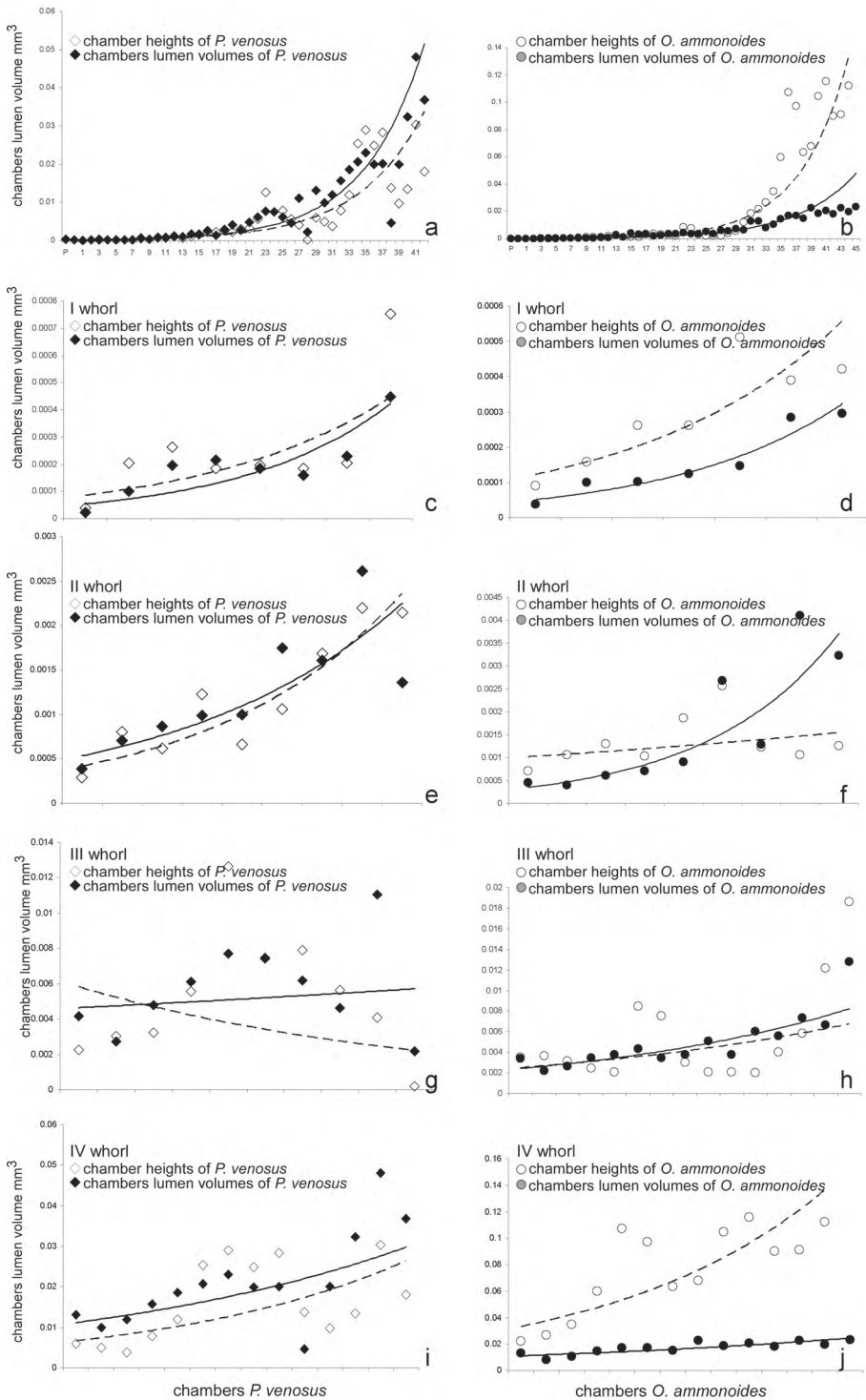
Figure 5. **(a)** Correspondence between chamber lumen volumes of *P. venosus* and septal lengths; **(b)** correspondence between chamber lumen volumes of *O. ammonoides* and septal lengths; **(c, e, g, i)** correspondence between chamber lumen volumes and septal lengths, whorl after whorl, of *P. venosus*; **(d, f, h, j)** correspondence between chamber lumen volumes and septal lengths, whorl after whorl, of *O. ammonoides*. Continuous lines are exponential functions for *P. venosus*; dashed lines are exponential functions for the *O. ammonoides*. All septal lengths were recalculated as the cubic power to make them comparable with volume.
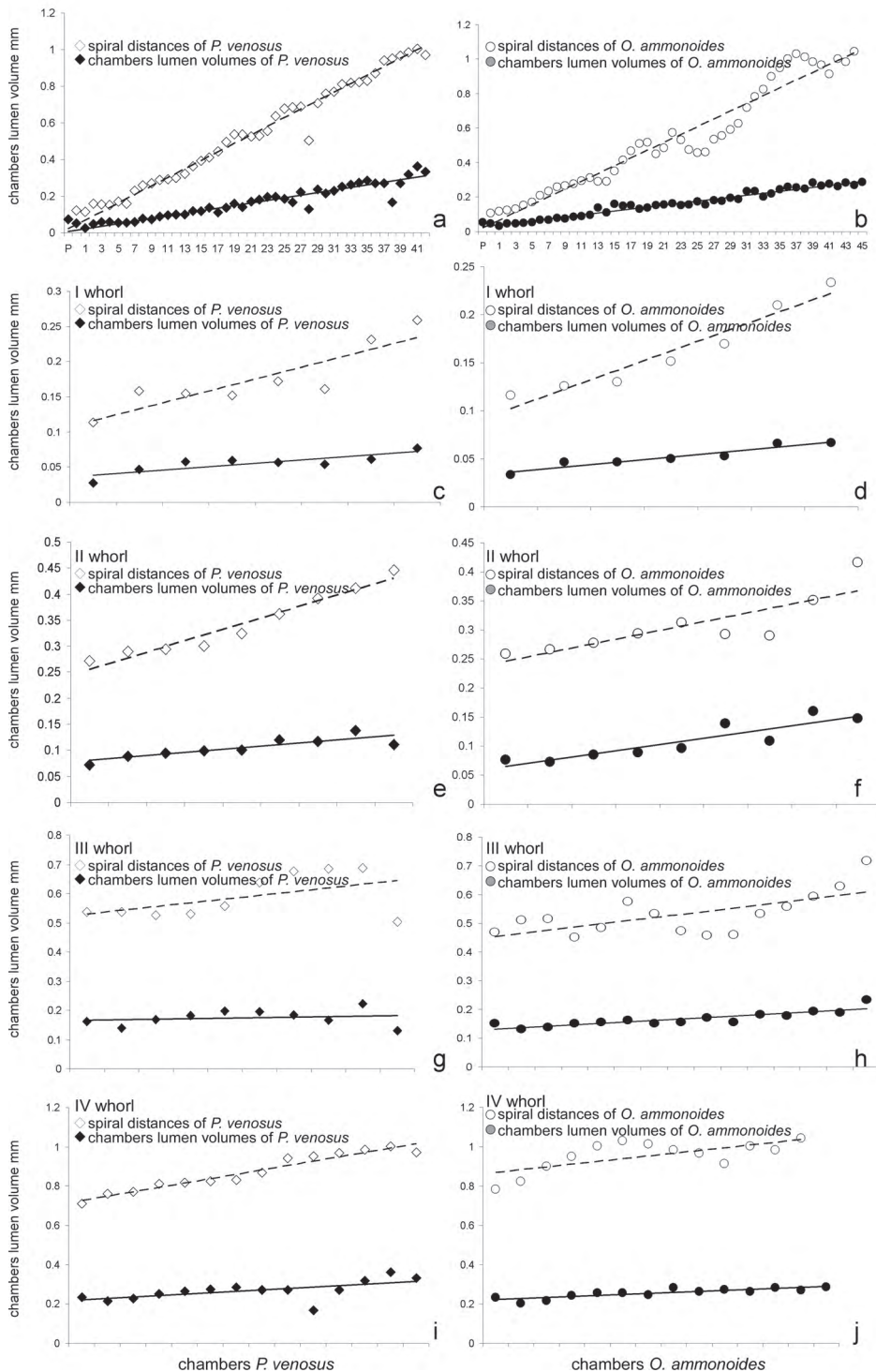
Figure 6. (a) Correspondence between chamber lumen volumes of *P. venosus* and chamber heights; **(b)** correspondence between chamber lumen volumes of *O. ammonoides* and chamber heights; **(c, e, g, i)** correspondence between chamber lumen volumes and chamber heights, whorl after whorl, of *P. venosus*; **(d, f, h, j)** correlation between chamber lumen volumes and chamber heights, whorl after whorl, of *O. ammonoides*. Continuous lines are exponential functions for *P. venosus*; dashed lines are exponential functions for *O. ammonoides*. All chamber heights were recalculated as the cubic power to make them comparable with volume.

694

Figure 7. (a) Correspondence between chamber lumen volumes of *P. venosus* and its spiral distances; (b) correspondence between chamber lumen volumes of *O. ammonoides* and its spiral distances; (c, e, g, i) corespondence between chamber lumen volumes and spiral distances, whorl after whorl, of *P. venosus*; (d, f, h, j) correspondence between chamber lumen volumes and spiral distances, whorl after whorl, of *O. ammonoides*. Continuous lines are linear functions for *P. venosus*; dashed lines are linear functions for *O. ammonoides*. All chamber lumen volumes were recalculated as the cubic root to make them comparable with spiral distances data.
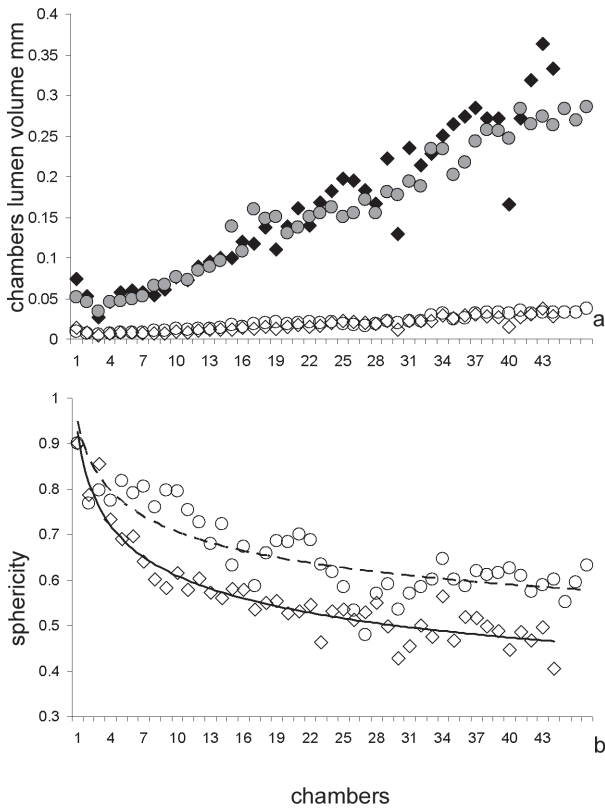
Figure 8. Deviations from sphericity: **(a)** correspondence between cubic root chamber lumen volumes and volume surface ratio. *P. venosus* chamber lumen volumes and volume surface ratios are represented by full and empty rhombuses; *O. ammonoides* chamber lumen volumes and volume surface ratios are represented by full and empty circles; **(b)** correspondence between sphericity deviation of *P. venosus* and *O. ammonoides* using the Wadell equation. Continuous line is the power function for *P. venosus*; dashed line is the power function for *O. ammonoides*.

Figure 9. Regression of chamber volume on the equatorial section area in *P. venosus* (full rhombuses) and *O. ammonoides* (empty circles). The regression functions are calculated as linear and power regression for *P. venosus* and as linear regression for *O. ammonoides*. Equations and coefficients of determination (R^2) are given.

are strictly limited by developmental genes and their interactions with the physico-chemical properties of the developing tissues (Newman & Müller 2000), in single celled foraminifera with a mineralised test. In nummulitids the form of the outer margin can be modelled by the equation

$$r = b_0(b_1 + b_2\theta)^\theta$$

where the length of the initial spiral (b_0), the expansion rate (b_1) and the acceleration rate (b_2) are constants (Hohenegger 2010). The parameter values are fixed for each individual, presumably as an inflexible part of their developmental genetics. Deviations from
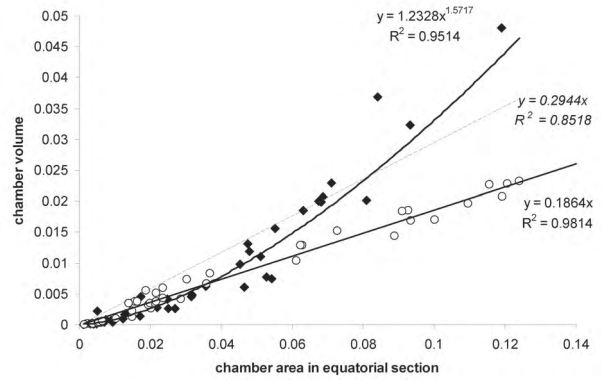
these fixed structures are caused by short but major environmental stress (such as extreme temperature or an attack by predator fish). Thickness, the second important character describing test and chamber shape, is also fixed, on the one hand by the connection with the radius, and on the other by parameters of the equation

$$th = b_0 \, r \, exp \, b_1$$

where b_0 represents the thickness constant and b_1 the allometric constant (Hohenegger 2010).

Every environmental stress can lead to a variation in volume growth rate. The chamber lumina, fixed by height (marginal radius) and thickness determined by genetic factors, can only react to stress by varying the septal distance during growth of the new wall.

Therefore, the mathematically infinite combinations of morphological solutions in building chambers with identical volumes are restricted by the verification limits of the character (e.g., negative numbers for test-wall thickness are impossible), degrees of freedom (e.g., dependence of septal distances from fixed marginal radius and thickness) and by the intensity and form of inter-correlations between characters based on gene and other regulatory interactions during development.

The study of the volume by 3D analysis gives a more complete idea of the specimen's growth

than do equatorially oriented thin sections. In thin sections, the chamber size in the operculinids seems to be generally bigger than in nummulitids; i.e., the chambers of operculinids are higher and the septal distance is bigger than in other nummulitids. In contrast, volume analysis shows that chambers of *P. venosus* reach the same size as *O. ammonoides* because the former is not as evolute as the latter. On Figure 3 some graphs are plotted showing the volume differences between the two specimens. The growth trend is comparable, and it is exponential at least for the first and the second whorl (Figure 3c, d). The last two whorls are not increasing as fast as the first ones and the very last chambers show no increase at all. Such trends, already shown three dimensionally by Speijer *et al.* (2008), reflect the achievement of reproduction in the adult stage. It is interesting that the chamber morphology is different in these two genera, but the chamber volumes are very similar. These differences at genus level, and above it, are not caused by ecological factors such as decreasing light intensities. The specimens studied here, belonging to two different genera, have similar shell thicknesses, despite living at different water depths, hinting at the underlying historical-phylogenetic background that is reflected in their inherited morphogenetic pathways.

In *O. ammonoides*, the chamber volume is achieved by extending the chamber height and by reducing alar prolongations; in contrast, the same volume is achieved in *P. venosus* by reducing the chamber height and by extending alar prolongations until the umbilical boss is reached. Thus, a similar biological need has been satisfied through two different developmental genetic solutions.

The three dimensional study of the embryo is also presented for these two species. The dimension of the proloculus is one of the main parameters in the taxonomy and systematics of larger foraminifera, and its dimension and position with respect to the deuteroloculus is characteristic in recognizing phylogenetic trends (Drooger 1993; Less *et al.* 2008). The deviation from sphericity in both proloculi is very low (close to 0.9) and they can be approximated as spheres. For these reasons, the traditional method of calculating only the largest diameter of the proloculus is representative for its volume.

The equatorial section can generally be considered as suitable for studying the ontogenesis in larger foraminifera, but according to our comparisons, the equatorial section character most consistent with the volume growth rate is the area. From the first whorl to the last one, the area growth rate gradually follows the volume data. As shown in Figure 9, the equatorial section area can be considered as well-suited to evaluate ontogeny in larger benthic foraminifera. The difference between evolute and involute forms is reflected in this figure.

In the involute *P. venosus* the equatorial section area of a chamber underestimates its actual volume. This underestimate increases with chamber growth and is caused by neglecting the alar prolongations, which are not visible in the equatorial section. In contrast, the constant evolute coiling of *O. ammonoides*, gives an accurate estimate of volume from the area using a constant multiplication factor.

Chamber length and height are only partially representative of the ontogenesis of the cell, mainly in the first two whorls.

Density calculation gives good results, although it is time-consuming for the extraction of all the hollow space within the marginal chord and septa, and requires very high image resolution. Nevertheless, such evaluation is useful in testing the calculation of density by mathematical formulae (Yordanova & Hohenegger 2007). In Nummulitidae, density values adopted in recent studies of hydrodynamics (Briguglio & Hohenegger 2009) or in palaeogeographic reconstruction (Jorry *et al.* 2006) are between 1.5 and 1.8 g/mm^3. The values obtained with this method also show significant differences between the two genera, and such differences can be explained partially by the different depositional environments to which they belong.

Conclusion

The detailed morphological and volumetric data obtained with 3D analysis indicate that the use of X-ray microtomography can be very useful for biometric research on foraminifera. Not only can intraspecific variation and evolutionary lineages be assessed or confirmed, based on the 3D shapes and sizes (Speijer *et al.* 2008), but such methodology can

be particularly advantageous for nummulitids where the growth rate and chamber geometry are the most important parameters for taxonomy, systematics and palaeobiology.

The calculation of volumes is important in studying the ontogenesis of the cell and can predict the reproduction stage or give details of the cell response to environmental changes through time (e.g., seasonality). The calculation of density can be used for prediction and evaluation of the hydrodynamic behaviour of nummulitids in the fossil record (Briguglio & Hohenegger 2009).

Further use of microCT scanning on larger benthic foraminifera is welcome because of the huge diversity of the group and because many hypotheses on evolution and phylogeny are based on classic 2D analysis and it would be interesting to test them on a three-dimensional scale.

Three-dimensional analyses of populations will also give much more information on volume variability and chamber morphologies, but today these procedures are too much time consuming.

However, we believe that the quantitative calculation of the shape, volume and growth rate of lumina may give a huge amount of information about the ontogenesis, palaeobiology, phylogeny, microevolution and taxonomy of larger benthic foraminifera.

All the relationships considered in this work indicate that not all the possible linear measurements on the equatorial section of a nummulitids are useful, at least for the last whorls in the adult stage. The calculation of the area, fast and precisely calculable with many computer programs, is more similar to the volume trend in every whorl and in the specimens studied here. Thus, area calculation might be considered especially useful for growth rate studies in thin section.

Acknowledgments

References

BLONDEAU, A. 1972. *Les Nummulites*, Librairie Vuibert 6d. Paris.

BRIGUGLIO, A. & HOHENEGGER, J. 2009. Nummulitids hydrodynamics: an example using *Nummulites globulus* Leymerie, 1846. *Bollettino della Società Paleontologica Italiana* **48**, 105–111.

CARLSON, W.D., ROWE, T., KETCHAM, R.A. & COLBERT, M.W. 2003. Application of high-resolution X-ray computed tomography in petrology, meteoritics and palaeontology. *In:* MEES, F., SWENNEN, R., VAN GEET, M. & JACOBS, P. (eds), *Applications of X-ray Computed Tomography in the Geosciences.* Geological Society, London, Special Publications **215**, 7–22.

DROOGER, C.W. 1993. Radial foraminifera: morphometrics and evolution. *Proceedings of the Koninklijke Nederlandse Akademie van Wetenschappen Series afd. Physics, eerste reeks* **41**.

FICHTEL, L. & MOLL, J.P.C. 1798. Testacea microscopica aliaque minuta ex generibus *Argonauta* et *Nautilus* ad naturam picta et descripta. *In*: RÖGL, F. & HANSEN, H.J. 1984. Foraminifera described by Fichtel & Moll in 1798, A revision of Testacea Microscopica. *Neue Denkschriften des Naturhistorischen Museums in Wien* **3**, 1–143.

GRONOVIUS, L.T. 1781. *Zoolphylacii Gronoviani. Exhibens vermes, Mollusca, Testacea et Zoophyta*. Theodorus Haak et Societe Leyden, 241–380.

HALLOCK, P. & GLENN, E.C. 1986. Larger foraminifera: a tool for paleoenvironmental analysis of Cenozoic carbonate depositional facies. *Palaios* **1**, 55–64.

HEMLEBEN, C., SPINDLER, M. & ANDERSON, O.R. 1989. *Modern Planktonic Foraminifera*. Springer, New York.

HOHENEGGER, J. 2011. Growth-invariant Meristic Characters. Tools to Reveal Phylogenetic Relationships in Nummulitidae (Foraminifera). *Turkish Journal of Earth Sciences* **20**, 665–681.

HOHENEGGER, J., YORDANOVA, E., NAKANO, Y. & TATZREITER, F. 1999. Habitats of larger foraminifera on the upper reef slope of Sesoko Island, Okinawa, Japan. *Marine Micropaleontology* **36**, 109–168.

HOTTINGER, L. 1977. Foraminiferes Operculiniformes. *Mémoires du Meséum National d'Histoire Naturelle.* Série C, Science del la terre, Tome XL.

HOTTINGER, L. 2009. The Paleocene and earliest Eocene foraminiferal Family Miscellaneidae: neither nummulitids nor rotaliids. *Carnet de Géologie / Notebooks on Geology, Brest*, Article 2006/06 (CG2009_A06).

JORRY, S., HASLER, C.A. & DAVAUD, E. 2006. Hydrodynamic behaviour of *Nummulites*: implications for depositional models. *Facies* **52**, 221–235.

LESS, G. & KOVACS, L. 1996. Age-estimates by European Paleogene Orthophragminae using numerical evolutionary correlation. *Geobios* **29**, 261–285.

LESS, G., ÖZCAN, E., PAPAZZONI, C.A. & STÖCKAR, R. 2008. The middle to late Eocene evolution of nummulitid foraminifer *Heterostegina* in the Western Tethys. *Acta Palaeontologica Polonica* **53**, 317–350.

METSCHER, B.D. 2009. MicroCT for comparative morphology: simple staining methods allow high-contrast 3D imaging of diverse non-mineralized tissues. *BMC Physiology* **9**, p. 11.

NEUES, F. & EPPLE, M. 2008. X-ray microcomputer tomography for the study of biomineralized endo- and exoskeletons of animals. *Chemical Reviews* **108**, 4734–4741.

NEWMAN, S.A. & MÜLLER, G.B. 2000. Epigenetic mechanisms of character origination. *Journal of Experimental Zoology* **288**, 304–317.

PAPAZZONI, C.A. 1998. Biometric analyses of *Nummulites 'ptukhiani'* Z.D. Kacharava, 1969 and *Nummulites fabianii* (Prever in fabiani, 1905). *Journal of Foraminiferal Research* **28**, 161–176.

PECHEUX, M.J.F. 1995. Ecomorphology of a recent large foraminifer, *Operculina ammonoides*. *Geobios* **28**, 529–566.

RACEY, A. 1992. The relative taxonomic value of morphological characters in the genus *Nummulites* (Foraminiferida). *Journal of Micropalaeontology* **11**, 197–209.

REISS, Z. & HOTTINGER, L. 1984. *The Gulf of Aqaba. Ecological Micropaleontology*. Springer-Verlag, Berlin.

ROVEDA, V. 1970. Revision of the Nummulites (Foraminiferida) of the *N. fabianii-fichteli* group. *Rivista italiana di Paleontologia* **76**, 235–324.

SCHAUB, H. 1981. *Nummulites et Assilines de la Tèthys paléogène. Taxinomie, phylogénese et biostratigraphie*. Mémoires Suisses de Paléontologie **104**–**106**.

SPEIJER, R.P., VAN LOO, D., MASSCHAELE, B., VLASSENBROECK, J., CNUDDE, V. & JACOBS, P. 2008. Quantifying foraminiferal growth with high-resolution X-ray computed tomography: new opportunities in foraminiferal ontogeny, phylogeny, and paleoceanography applications. *Geosphere* **4**, 760–763.

WADELL, H. 1932. Volume, shape and roundness of rock particles. *Journal of Geology* **40**, 443–451.

YORDANOVA, E. & HOHENEGGER, J. 2007. Studies on settling, traction and entrainment of larger benthic foraminiferal tests: implication for accumulation in shallow marine sediments. *Sedimentology* **54**, 1273–1306.